Biochimica et Biophysica Acta 1798 (2010) 1056–1061

Contents lists available at ScienceDirect

Biochimica et Biophysica Acta

journal homepage: www.elsevier.com/locate/bbamem

# Membrane interaction of the N-terminal domain of chemokine receptor CXCR1

Sourav Haldar [a,1], H. Raghuraman [a,1,2], Trishool Namani [a], Krishna Rajarathnam [b], Amitabha Chattopadhyay [a,*]

[a] Centre for Cellular and Molecular Biology, Council of Scientific and Industrial Research, Uppal Road, Hyderabad 500 007, India

[b] Department of Biochemistry and Molecular Biology, Sealy Center for Structural Biology and Molecular Biophysics, the University of Texas Medical Branch, Galveston, TX 77555-1055, USA

ARTICLE INFO

*Article history:*
Received 15 August 2009
Received in revised form 22 February 2010
Accepted 26 February 2010
Available online 11 March 2010

*Keywords:*
Chemokine receptor
G-protein coupled receptor
Surface pressure
Red edge excitation shift
Membrane vesicle
Lipid monolayer

ABSTRACT

The N-terminal domain of chemokine receptors constitutes one of the two critical ligand binding sites, and plays important roles by mediating binding affinity, receptor selectivity, and regulating function. In this work, we monitored the organization and dynamics of a 34-mer peptide of the CXC chemokine receptor 1 (CXCR1) N-terminal domain and its interaction with membranes by utilizing a combination of fluorescence-based approaches and surface pressure measurements. Our results show that the CXCR1 N-domain 34-mer peptide binds vesicles of 1,2-dioleoyl-*sn*-glycero-3-phosphocholine (DOPC) and upon binding, the tryptophan residues of the peptide experience motional restriction and exhibit red edge excitation shift (REES) of 19 nm. These results are further supported by increase in fluorescence anisotropy and mean fluorescence lifetime upon membrane binding. These results constitute one of the first reports demonstrating membrane interaction of the N-terminal domain of CXCR1 and gain relevance in the context of the emerging role of cellular membranes in chemokine signaling.



## 1. Introduction

Chemokines (chemotactic cytokines) are a large family of small soluble proteins (70–120 residues) and play a crucial regulatory role in innate immunity, inflammation, host defense against infection, embryogenesis and metastasis [1,2]. They are classified either as CC, CXC, CX3C, or C based on the presence of conserved cysteine residues near the N-terminus. Chemokines elicit transmembrane signaling by activation of a subclass of G-protein coupled receptors (GPCRs). Although the chemokine receptor family is the largest subfamily of peptide-binding GPCRs [3], the structures of chemokine receptors are not known. This is due to the fact that very few crystal structures of GPCRs are available because of intrinsic difficulties of determining membrane-embedded protein structures [4]. For this reason, approaches based on fluorescence spectroscopy have often proved useful in elucidating the organization, topology and orientation of GPCRs [5].

A variety of studies using chimeras and mutagenesis have shown that the extracellular N-terminal domain of chemokine receptors plays critical roles in determining binding affinity, receptor selectivity, and also in regulating signaling activities [1,6]. In order to understand the role of the N-terminal domain in ligand specificity and affinity of CXCR1, the organization and dynamics of the CXCR1 N-domain were earlier studied in micellar environments [7]. This study showed that the CXCR1 N-terminal domain adopts a defined conformation (secondary structure) in dodecylphosphocholine (DPC) micelles suggesting that the cellular membrane may play an important role in regulating CXCR1 function. Although micelles are used as membrane-mimetics [8], they are limited as membrane models due to their intrinsic curvature stress, small size and lack of appropriate interface [9]. In this paper, we have monitored the organization and dynamics of the CXCR1 N-domain (see Fig. 1) in the presence of membranes by utilizing a combination of fluorescence-based measurements including red edge excitation shift (REES) [10], and surface pressure measurements.

## 2. Materials and methods

### 2.1. Materials

1,2-Dimyristoyl-*sn*-glycero-3-phosphocholine (DMPC) and 3-(N-morpholino) propanesulfonicacid (MOPS) were obtained from Sigma Chemical Co. (St. Louis, MO). 1,2-Dioleoyl-*sn*-glycero-3-phosphocholine (DOPC) and DPC were purchased from Avanti Polar Lipids (Alabaster, AL). The purity of DOPC was checked by thin layer

*Abbreviations:* CXCR1, CXC chemokine receptor 1; DMPC, 1,2-dimyristoyl-*sn*-glycero-3-phosphocholine; DOPC, 1,2-dioleoyl-*sn*-glycero-3-phosphocholine; DPC, dodecylphosphocholine; GPCR, G-protein coupled receptor; LUV, large unilamellar vesicle; MOPS, 3-(N-morpholino)propanesulfonic acid; REES, red edge excitation shift

* Corresponding author. Tel.: +91 40 2719 2578; fax: +91 40 2716 0311.
*E-mail address:* amit@ccmb.res.in (A. Chattopadhyay).

[1] These authors contributed equally to the work.

[2] Present address: Department of Biochemistry and Molecular Biology, Centre for Integrative Sciences, the University of Chicago, 929 East 57th Street, Chicago, IL 60637, USA.

0005-2736/$ – see front matter © 2010 Elsevier B.V. All rights reserved.
doi:10.1016/j.bbamem.2010.02.029

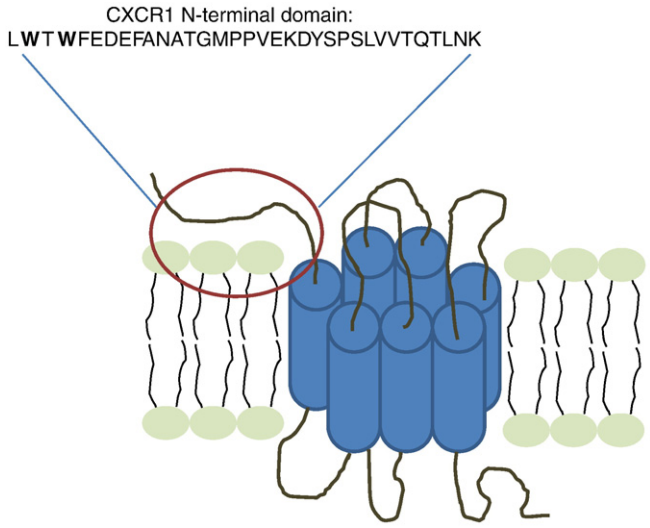


**Fig. 1.** A schematic representation of the CXCR1 receptor. The N-terminal domain (whose sequence is shown) is implicated in ligand binding and signal specificity. The sequence of the rabbit CXCR1 N-domain is shown (the tryptophan residues are highlighted). The construct shown lacks 10 amino acids at the N-terminal end and this stretch of amino acids has previously been shown to be not essential for ligand binding (see ref. [7] for more details). In this study, we have monitored the interaction of CXCR1 N-terminal domain 34-mer peptide with membranes. As a negative control, a peptide with identical amino acid composition but with a scrambled sequence was used. See Materials and methods for other details.

chromatography on silica gel precoated plates (Merck) in chloroform/methanol/water (65:35:5, v/v/v) and was found to give only one spot with a phosphate-sensitive spray and on subsequent charring [11]. Concentration of DOPC was determined by phosphate assay subsequent to total digestion by perchloric acid [12]. DMPC was used as an internal standard. Water was purified through a Millipore (Bedford, MA) Milli-Q system and used throughout. N-domain CXCR1 peptides were synthesized as described previously [7].

## 2.2. Methods

### 2.2.1. Sample preparation

In this study, we have monitored the interaction of an N-terminal CXCR1 N-domain peptide with membranes, and as a negative control, we have used a peptide with identical amino acid composition but with a scrambled sequence. The sequences are shown below:

CXCR1 N-domain 34mer LWTWFEDEFANATGMPPVEKDYSPSLVVTQTLNK
Scrambled peptide DVPLSTSATEGKTAWDKQVMLFTLPNEYFNVWPE

Fluorescence measurements were performed using large unilamellar vesicles (LUVs) of 100 nm diameter of DOPC. In general, 640 nmol of DOPC was dried under a stream of nitrogen while being warmed gently (~35 °C). After further drying under a high vacuum for at least 3 h, the lipid film was hydrated (swelled) by adding 1.5 ml of 10 mM MOPS, pH 7.4 buffer, and was vortexed for 3 min to uniformly disperse the lipid and form homogeneous multilamellar vesicles. LUVs of 100 nm diameter were prepared by the extrusion technique using an Avestin Liposofast Extruder (Ottawa, Ontario, Canada) as previously described [13]. Briefly, the multilamellar vesicles were freeze-thawed five times using liquid nitrogen to ensure solute equilibration between trapped and bulk solutions, and then extruded through polycarbonate filters (pore diameter of 100 nm) mounted in the extruder fitted with Hamilton syringes (Hamilton Company, Reno, NV). The samples were subjected to 11 passes through polycarbonate filters to give the final LUV suspension. In order to incorporate CXCR1 peptides (34-mer and scrambled) into membranes, a small aliquot containing 1.28 nmol of the peptide from a stock solution in water was added to the preformed vesicles and mixed well to give membranes containing 0.2 mol% peptide. Background samples were prepared the same way except that peptides were not added to them. Samples were kept in the dark for 12 h before measuring fluorescence. All experiments were performed with multiple sets of samples at room temperature (~23 °C).

### 2.2.2. Steady state fluorescence measurements

Steady state fluorescence measurements were performed with a Hitachi F-4010 spectrofluorometer using 1 cm pathlength quartz cuvettes. Excitation and emission slits with a nominal bandpass of 5 nm were used for all measurements. All spectra were recorded in the correct spectrum mode. Background intensities of samples were subtracted from each sample spectrum to cancel out any contribution due to the solvent Raman peak and other scattering artifacts. The spectral shifts obtained with different sets of samples were identical in most cases. In other cases, the values were within ±1 nm of the ones reported. Fluorescence anisotropy measurements were performed at room temperature (~23 °C) using a Hitachi polarization accessory. Anisotropy values were calculated from the equation [14]:

$$r = \frac{I_{VV} - GI_{VH}}{I_{VV} + 2GI_{VH}} \quad (1)$$

where $I_{VV}$ and $I_{VH}$ are the measured fluorescence intensities (after appropriate background subtraction) with the excitation polarizer oriented vertically and the emission polarizer vertically and horizontally oriented, respectively. $G$ is the grating correction factor that corrects for wavelength-dependent distortion of the polarizers and is the ratio of the efficiencies of the detection system for vertically and horizontally polarized light, and is equal to $I_{HV}/I_{HH}$. All experiments were done with multiple sets of samples and average values of anisotropy are shown in Fig. 5.

### 2.2.3. Surface pressure measurements

Monolayer studies were performed at room temperature (~23 °C) using a Langmuir–Blodgett equipment (NIMA technology, Model 611MC, Coventry, U.K.), with a computer-controlled multi-compartment surface area (dimensions 15 cm × 10 cm) with two mechanically coupled barriers. Mili-Q water was used as the subphase and the total volume of the subphase was 75 ml. DOPC was deposited from a methanol stock solution on the subphase. Methanol was allowed to evaporate and the monolayer was continuously compressed with symmetrical barriers at a constant speed of 30 $cm^2$/min up to its collapse pressure. Peptides were introduced into the subphase with a syringe after forming the lipid monolayer at an initial surface pressure of 15 mN/m. The subphase was continuously stirred. Surface pressure was monitored by the Wilhelmy method using a paper plate in conjunction with a microbalance. In order to monitor the interaction of CXCR1 peptides with DOPC monolayers, increase in surface pressure as a function of time was monitored using NIMA software for a given initial pressure at constant area.

### 2.2.4. Time-resolved fluorescence measurements

Fluorescence lifetimes were calculated from time-resolved fluorescence intensity decays using IBH 5000F coaxial nanosecond flash lamp equipment (Horiba Jobin Yvon, Edison, NJ) with DataStation software in the time-correlated single photon counting mode. This machine uses a thyratron-gated nanosecond flash lamp filled with nitrogen as the plasma gas (~1 bar) and is run at 40 kHz. Lamp profiles were measured at the excitation wavelength using Ludox (colloidal silica) as the scatterer. To optimize the signal to noise ratio, 5000 photon counts were collected in the peak channel. All experiments were performed using excitation and emission slits with a bandpass of 8 nm. The sample and the scatterer were

alternated after every 10% acquisition to ensure compensation for shape and timing drifts occurring during the period of data collection. This arrangement also prevents any prolonged exposure of the sample to the excitation beam, thereby avoiding any possible photodamage of the fluorophore. Data were stored and analyzed using DAS 6.2 software (Horiba Jobin Yvon). Fluorescence intensity decay curves so obtained were deconvoluted with the instrument response function and analyzed as a sum of exponential terms:

$$F(t) = \sum_i \alpha_i \exp(-t/\tau_i) \quad (2)$$

where $F(t)$ is the fluorescence intensity at time $t$ and $\alpha_i$ is a pre-exponential factor representing the fractional contribution to the time-resolved decay of the component with a lifetime $\tau_i$ such that $\Sigma_i \alpha_i = 1$. The program also includes statistical and plotting subroutine packages [15]. The goodness of the fit of a given set of observed data and the chosen function was evaluated by the $\chi^2$ ratio, the weighted residuals [16], and the autocorrelation function of the weighted residuals [17]. A fit was considered acceptable when plots of the weighted residuals and the autocorrelation function showed random deviation about zero with a minimum $\chi^2$ value not more than 1.4. Intensity-averaged mean lifetimes $<\tau>$ for biexponential decays of fluorescence were calculated from the decay times and pre-exponential factors using the following equation [14]:

$$\tau = \frac{\alpha_1\tau_1^2 + \alpha_2\tau_2^2}{\alpha_1\tau_1 + \alpha_2\tau_2}. \quad (3)$$

## 3. Results and discussion

### 3.1. Fluorescence characteristics and membrane binding of the CXCR1 N-terminal domain peptide

It is now well established that chemokine binding and function involves two regions of the ligand and two regions of the receptors — interactions between chemokine N-loop and receptor N-domain residues (site-I), and between chemokine N-terminal and receptor extracellular/transmembrane residues (site-II). The site-I interaction plays multiple roles and mediates binding affinity and receptor selectivity, and regulates signaling functions [1,6]. In this work, we have used fluorescence-based approaches to probe membrane interactions of a CXCR1 N-terminal domain 34-mer peptide. The fluorescence emission spectra of the CXCR1 N-domain peptide (sequence shown in Fig. 1) in buffer and when bound to DOPC vesicles are shown in Fig. 2a. As a negative control, a scrambled peptide with identical amino acid composition was used (sequences of both peptides are shown in Materials and methods). The scrambled sequence was generated using a random sequence generator from the web tool: http://www.expasy.ch/tools/randseq.html. In addition, we manually checked to ensure that there was no overlap with the native sequence and that there were no clusters of hydrophobic or charged amino acids.

The maximum of fluorescence emission[3] of the tryptophan residues in the CXCR1 N-domain peptide in buffer is 350 nm. In the presence of DOPC vesicles, the CXCR1 N-domain peptide exhibits a blue shifted (*i.e.*, toward shorter wavelength) emission maximum at 344 nm, indicating a less polar environment around the tryptophan residues, due to binding of the peptide to membranes. On the other hand, the scrambled peptide did not show any change in the wavelength of maximum fluorescence emission in the presence of DOPC vesicles, thereby indicating lack of appreciable binding to membranes.

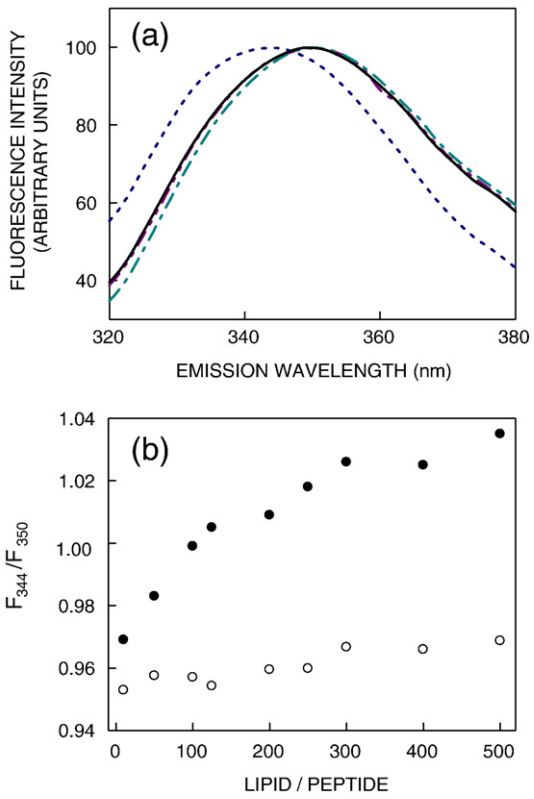


**Fig. 2.** (a) Fluorescence emission spectra of the CXCR1 N-domain and scrambled peptides: the CXCR1 N-domain in buffer (———, black) and DOPC vesicles (— — —, blue); scrambled peptide in buffer (– – – –, cyan) and DOPC vesicles (– – – – –, purple). The scrambled peptide refers to a peptide with identical amino acid composition but with scrambled sequence (see text for details). Spectra are intensity-normalized at the respective emission maxima. Measurements were carried out at room temperature (~23 °C). The excitation wavelength used was 280 nm. The ratio of peptide to lipid was 1:500 (mol/mol) and lipid concentration was 0.43 mM in all cases. (b) Binding of the CXCR1 N-domain (●) and scrambled peptide (○) to DOPC vesicles measured by the changes in peptide fluorescence. The ratio of fluorescence intensity monitored at 344 and 350 nm is plotted as function of lipid/peptide ratio. The concentration of peptide was 0.85 μM in all cases. See Materials and methods for other details.

The membrane binding of the CXCR1 N-domain peptide can be quantitated by the blue shift of emission maximum (from 350 to 344 nm) upon binding to DOPC vesicles and can be attributed to the change in polarity of the surrounding environment. The increase in the fluorescence intensity ratio ($F_{344}/F_{350}$) therefore represents the fraction of membrane-bound peptide. Fig. 2b shows the binding curve for the CXCR1 N-domain peptide to DOPC vesicles monitored in this fashion. The fluorescence intensity ratio gradually increases with increasing with lipid/peptide ratio (mol/mol) and reaches a maximum value at lipid/peptide ratio of ~500. Importantly, the fluorescence intensity ratio remains invariant in case of the scrambled peptide, indicating that membrane binding of the N-terminal domain is sequence-specific and not dependent on the overall hydrophobicity. We chose conditions for our experiments to ensure that the CXCR1 N-domain peptide is predominantly membrane-bound, *i.e.*, there is no ground state heterogeneity.

### 3.2. Monolayer studies with the CXCR1 N-domain peptide

In order to monitor the interaction of the CXCR1 N-domain peptide with membranes, we explored the interaction of the peptide with DOPC monolayer. The monolayer technique represents a useful

[3] We have used the term maximum of fluorescence emission in a somewhat wider sense here. In every case, we have monitored the wavelength corresponding to maximum fluorescence intensity, as well as the center of the mass of the fluorescence emission. In most cases, both these methods yielded the same wavelength. In cases where minor discrepancies were found, the center of mass of emission has been reported as the fluorescence maximum.

approach to study lipid–peptide interactions [18,19]. Insertion of peptides into lipid monolayers can be studied by monitoring the increase in surface pressure at a constant area as a function of time. Fig. 3 shows the increase in surface pressure of DOPC monolayer with time when the CXCR1 N-domain peptide was injected in the sub phase. The increase in surface pressure with time is indicative of specific binding of the CXCR1 N-domain peptide to DOPC monolayer. In contrast, the increase in surface pressure is much less pronounced for the scrambled peptide.

### 3.3. Red edge excitation shift (REES) of membrane-bound CXCR1 N-domain peptide

REES represents a powerful approach that can be used to directly monitor the environment and dynamics around a fluorophore in complex biological systems [10,20,21]. A shift in the wavelength of maximum fluorescence emission toward higher wavelengths, caused by a shift in the excitation wavelength toward the red edge of the absorption band, is termed REES. This effect is mostly observed with polar fluorophores in motionally restricted environments where the dipolar relaxation time for the solvent shell around a fluorophore is comparable to or longer than its fluorescence lifetime. We have previously shown that REES serves as a sensitive tool to monitor the organization and dynamics of membrane-bound peptides [22].

The shift in the maximum of fluorescence emission of the tryptophans of the CXCR1 N-domain peptide bound to DOPC vesicles as a function of excitation wavelength is shown in Fig. 4. As the excitation wavelength is changed from 280 to 307 nm, the emission maximum of membrane-bound CXCR1 N-domain peptide is shifted from 344 to 363 nm that corresponds to REES of 19 nm. It is possible that there could be further red shift if excitation is carried out beyond 310 nm. We found it difficult to work in this wavelength range due to low signal to noise ratio and artifacts due to the solvent Raman peak that sometimes remained even after background subtraction. Such dependence of the emission maximum on excitation wavelength is characteristic of REES. This implies that the tryptophan residues in the CXCR1 N-domain peptide are localized in a motionally restricted region of the membrane. It is worth mentioning here that the magnitude of REES obtained in the case of membrane-bound CXCR1 N-domain peptide is considerably higher than what is usually reported for membrane-bound tryptophan residues [22–24], although higher REES has been reported in a few cases [25,26]. In a control

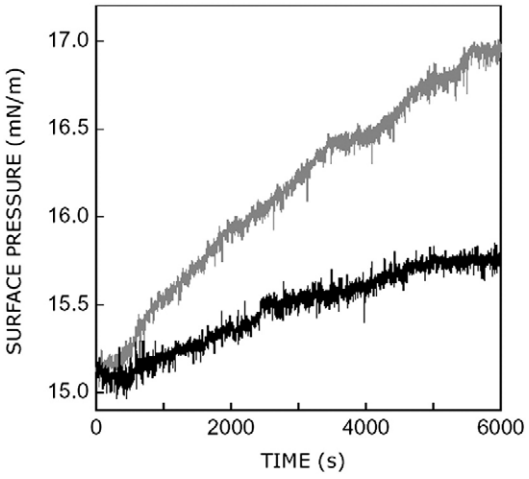


**Fig. 3.** Interaction of the CXCR1 N-domain and scrambled peptides with DOPC monolayer. The initial surface pressure was ~15 mN/m. Change in surface pressure with time was recorded. The gray and black lines represent the increase in surface pressure for the CXCR1 N-domain and the scrambled peptide, respectively. Measurements were carried out with 16 nmol lipid at room temperature (~23 °C). See Materials and methods for other details.

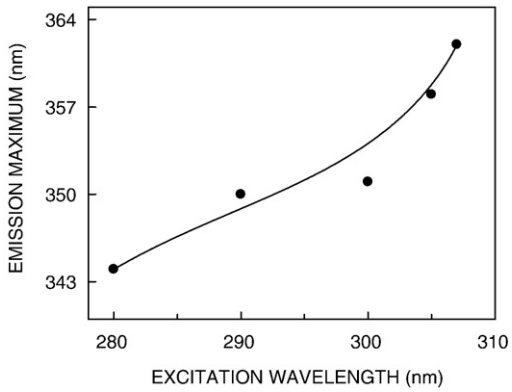


**Fig. 4.** Effect of changing excitation wavelength on the wavelength of maximum emission for the CXCR1 N-domain peptide in DOPC vesicles. The ratio of peptide to lipid was 1:500 (mol/mol) and lipid concentration was 0.43 mM. The line joining the data points is provided merely as a viewing guide. See Materials and methods for other details.

experiment, we observed that the CXCR1 N-domain peptide exhibits a nominal REES of 9 nm in buffer (relative to 19 nm in case of membrane-bound peptide; see Fig. S1 in Supplementary material). The scrambled peptide, on the other hand, displays similar REES in buffer and in the presence of DOPC vesicles (Fig. S1 in Supplementary material). In DPC micelles, the CXCR1 N-domain peptide shows REES of 13 nm (see Fig. S2a in Supplementary material). The reduced magnitude of REES could be due to curvature stress or lack of proper interface in micelles as described above.

We interpret this restriction in tryptophan environment to the binding of the CXCR1 N-domain peptide to DOPC membranes. The membrane interface is characterized by unique motional and dielectric characteristics, distinct from the bulk aqueous phase and the more isotropic hydrocarbon-like deeper regions of the membrane [10]. This specific region of the membrane exhibits slow rates of solvent relaxation and is also known to participate in intermolecular charge interactions and hydrogen bonding through the polar headgroup. These structural features, which slow down the rate of solvent reorientation, have previously been recognized as typical features of microenvironments giving rise to significant REES effects. It is therefore the membrane interface that is most likely to display red edge effects.

### 3.4. Fluorescence anisotropy and lifetime of the CXCR1 N-domain peptide

The steady state fluorescence anisotropy of tryptophans of the CXCR1 N-domain peptide in buffer and DOPC vesicles are shown in Fig. 5. As shown in the figure, the anisotropy of the CXCR1 N-domain peptide exhibits an increase in the presence of DOPC vesicles. This increase in anisotropy could be interpreted as the reduction in rotational mobility of tryptophans due to binding of the peptide to DOPC membranes. The increase in anisotropy reinforces the motionally restricted environment experienced by the tryptophans upon binding to membranes. The fluorescence anisotropy of the CXCR1 N-domain peptide in DPC micelles is shown in Fig. S2b (see Supplementary material).

**Table 1**
Fluorescence lifetimes of the CXCR1 N-domain peptide[a].

| Condition | $\alpha_1$ | $\tau_1$ (ns) | $\alpha_2$ | $\tau_2$ (ns) |
|---|---|---|---|---|
| Buffer | 0.69 | 1.11 | 0.31 | 3.74 |
| DOPC vesicles | 0.56 | 1.04 | 0.44 | 5.21 |

[a] The excitation wavelength was 295 nm; emission was monitored at 350 and 344 nm in buffer and DOPC vesicles, respectively. All other conditions are as in Fig. 2. See Materials and methods for other details.

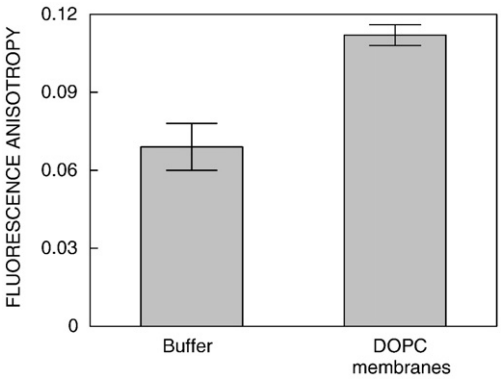


**Fig. 5.** Steady state fluorescence anisotropy of the CXCR1 N-domain peptide in buffer and DOPC vesicles. The excitation wavelength used was 295 nm. Emission was monitored at 350 and 344 nm in case of buffer and DOPC vesicles, respectively. Data shown are means ± S.E. of at least three independent measurements. All other conditions are as in Fig. 2. See Materials and methods for other details.

Fluorescence lifetime serves as a faithful indicator of the local environment in which a given fluorophore is placed [27]. In general, tryptophan lifetimes are known to be reduced when exposed to polar environments [28]. A typical decay profile of the CXCR1 N-domain peptide in buffer with its biexponential fitting and the statistical parameters used to check the goodness of the fit is shown in Fig. 6a. Table 1 shows the tryptophan lifetimes for the CXCR1 N-domain peptide in buffer and DOPC vesicles. All fluorescence decays could be fitted with a biexponential function. We chose to use the intensity-averaged mean fluorescence lifetime as an important parameter since it is independent of the method of analysis and the number of exponentials used to fit the time-resolved fluorescence decay. The mean fluorescence lifetime was calculated using Eq. (3). Fig. 6b shows that the mean fluorescence lifetime of tryptophans in the CXCR1 N-domain peptide in buffer is ~2.7 ns. The lifetime increases to ~4.4 ns in the presence of DOPC vesicles. The increase in mean fluorescence lifetime could be due to the reduced polarity experienced by the CXCR1 N-domain tryptophans upon binding to DOPC membranes [28]. Interestingly, the mean fluorescence lifetime of the CXCR1 N-domain peptide in DPC micelles is somewhat shorter, possibly due to increased water penetration (see Fig. S2c in Supplementary material).

Chemokine receptors belong to the GPCR superfamily of receptors. The GPCR superfamily is the largest and most diverse protein family in mammals, involved in signal transduction across membranes [29]. GPCRs mediate multiple physiological processes such as neurotransmission, cellular metabolism, secretion, cellular differentiation, growth, inflammatory and immune responses. For this reason, GPCRs have emerged as major targets for the development of novel drug candidates in all clinical areas [30]. Yet, exploring structure–function relationships of GPCRs poses considerable challenge since very few crystal structures of GPCRs are available [4]. This is due to the inherent difficulty in crystallizing membrane proteins in their native conditions because of their intrinsic dependence on surrounding membrane lipids [31]. In this overall context, monitoring organization of the functionally important domains, such as illustrated in this study for a chemokine receptor N-terminal domain peptide and its interaction with membranes using fluorescence-based approaches assume relevance.

In this paper, we explored the organization and dynamics of the CXCR1 N-terminal domain in the membrane milieu. Our results, utilizing intrinsic fluorescence of tryptophans and monolayer studies, show that the CXCR1 N-domain preferentially interacts with membranes. To the best of our knowledge, this is the very first report showing interaction of functionally important N-terminal domain of any chemokine receptor with membrane bilayers. We report that upon binding to membranes, the tryptophan residues of the CXCR1 N-domain experience motional restriction and exhibit REES. This is further supported by increase in fluorescence anisotropy and mean fluorescence lifetime upon membrane binding. This motional restriction could result in loss of conformational entropy and therefore likely to influence ligand binding properties of the receptor. These results assume significance in view of the role of chemokine receptors in a number of inflammatory diseases and cancer [3,32], and the emerging paradigm that cellular membranes could be important modulators of chemokine receptors.

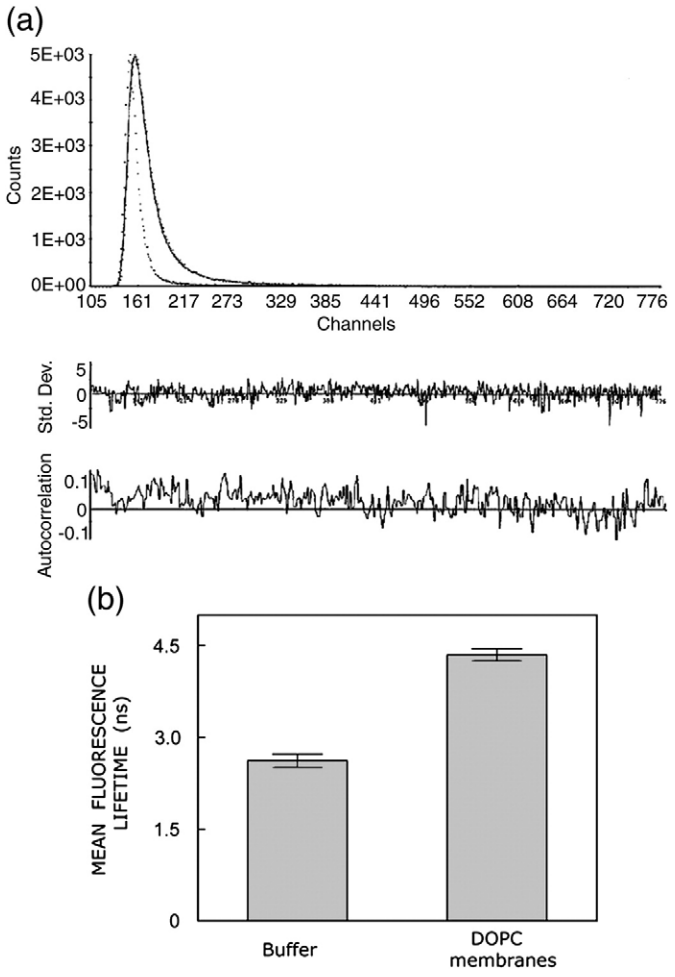


**Fig. 6.** (a) Representative time-resolved fluorescence intensity decay of the CXCR1 N-domain peptide in buffer. The excitation wavelength was 295 nm which corresponds to a peak in the spectral output of the nitrogen lamp. Emission was monitored at 350 nm. The sharp peak on the left is the lamp profile. The relatively broad peak on the right is the decay profile, fitted to a biexponential function. The two lower plots show the weighted residuals and the autocorrelation function of the weighted residuals. (b) Mean fluorescence lifetime of the CXCR1 N-domain peptide in buffer and DOPC membranes. The excitation wavelength was 295 nm. Emission was monitored at 350 and 344 nm in case of buffer and DOPC vesicles, respectively. Mean fluorescence lifetimes were calculated from Table 1 using Eq. (3). Measurements were carried out at room temperature (~23 °C). Data shown are means ± S.E. of at least three independent measurements. All other conditions are as in Fig. 2. See Materials and methods for other details.

## Acknowledgements

This work was supported by research grants from the Council of Scientific and Industrial Research, Government of India (A.C.) and NIH grant R21-AI058776 (K.R.). S.H. thanks the Council of Scientific and Industrial Research for the award of a Senior Research Fellowship. H.R. and T.N. thank the Council of Scientific and Industrial Research and Life Science Research Board for the award of Postdoctoral Fellowships. A.C. is an Adjunct Professor at the Special Centre for Molecular Medicine of

Jawaharlal Nehru University (New Delhi, India), and an Honorary Professor of the Jawaharlal Nehru Centre for Advanced Scientific Research (Bangalore, India). A.C. gratefully acknowledges J.C. Bose Fellowship (Department of Science and Technology, Government of India). We thank members of A.C's research group for critically reading the manuscript.

## Appendix A. Supplementary data

Supplementary data associated with this article can be found, in the online version, at doi:10.1016/j.bbamem.2010.02.029.

## References

[1] L. Rajagopalan, K. Rajarathnam, Structural basis of chemokine receptor function — a model for binding affinity and ligand selectivity, Biosci. Rep. 26 (2006) 325–329.
[2] S.J. Allen, S.E. Crown, T.M. Handel, Chemokine: receptor structure, interactions, and antagonism, Annu. Rev. Immunol. 25 (2007) 787–820.
[3] J.J. Onuffer, R. Horuk, Chemokines, chemokine receptors and small-molecule antagonists: recent developments, Trends Pharmacol. Sci. 23 (2002) 459–467.
[4] M.A. Hanson, R.C. Stevens, Discovery of new GPCR biology: one receptor structure at a time, Structure 17 (2009) 8–14.
[5] A. Chattopadhyay, H. Raghuraman, Application of fluorescence spectroscopy to membrane protein structure and dynamics, Curr. Sci. 87 (2004) 175–180.
[6] G.N. Prado, K. Suetomi, D. Shumate, C. Maxwell, A. Ravindran, K. Rajarathnam, J. Navarro, Chemokine signaling specificity: essential role for the N-terminal domain of chemokine receptors, Biochemistry 46 (2007) 8961–8968.
[7] L. Rajagopalan, K. Rajarathnam, Ligand selectivity and affinity of chemokine receptor CXCR1, J. Biol. Chem. 279 (2004) 30000–30008.
[8] S.S. Rawat, A. Chattopadhyay, Structural transition in the micellar assembly: a fluorescence study, J. Fluoresc. 9 (1999) 233–244.
[9] S. Mukherjee, A. Chattopadhyay, Motionally restricted tryptophan environments at the peptide–lipid interface of gramicidin channels, Biochemistry 33 (1994) 5089–5097.
[10] A. Chattopadhyay, Exploring membrane organization and dynamics by the wavelength-selective fluorescence approach, Chem. Phys. Lipids 122 (2003) 3–17.
[11] J.C. Dittmer, R.L. Lester, A simple, specific spray for the detection of phospholipids on thin-layer chromatograms, J. Lipid Res. 5 (1964) 126–127.
[12] C.W.F. McClare, An accurate and convenient organic phosphorus assay, Anal. Biochem. 39 (1971) 527–530.
[13] R.C. MacDonald, R.I. MacDonald, B.P. Menco, K. Takeshita, N.K. Subbarao, L.R. Hu, Small-volume extrusion apparatus for preparation of large, unilamellar vesicles, Biochim. Biophys. Acta 1061 (1991) 297–303.
[14] J.R. Lakowicz, Principles of Fluorescence Spectroscopy, 3rd ed.Springer, New York, 2006.
[15] D.V. O'Connor, D. Phillips, Time-Correlated Single Photon Counting, Academic Press, London, 1984, pp. 180–189.
[16] R.A. Lampert, L.A. Chewter, D. Phillips, D.V. O'Connor, A.J. Roberts, S.R. Meech, Standards for nanosecond fluorescence decay time measurements, Anal. Chem. 55 (1983) 68–73.
[17] A. Grinvald, I.Z. Steinberg, On the analysis of fluorescence decay kinetics by the method of least-squares, Anal. Biochem. 59 (1974) 583–598.
[18] R. Maget-Dana, The monolayer technique: a potent tool for studying the interfacial properties of antimicrobial and membrane-lytic peptides and their interactions with lipid membranes, Biochim. Biophys. Acta 1462 (1999) 109–140.
[19] V. Krishnakumari, R. Nagaraj, Interaction of antimicrobial peptides spanning the carboxy-terminal region of human β-defensins 1–3 with phospholipids at the air–water interface and inner membrane of E. coli, Peptides 29 (2008) 7–14.
[20] A.P. Demchenko, Site-selective red-edge effects, Methods Enzymol. 450 (2008) 59–78.
[21] H. Raghuraman, D.A. Kelkar, A. Chattopadhyay, Novel insights into protein structure and dynamics utilizing the red edge excitation shift approach, in: C.D. Geddes, J.R. Lakowicz (Eds.), Reviews in Fluorescence 2005, vol. 2, Springer, New York, 2005, pp. 199–224.
[22] S.S. Rawat, D.A. Kelkar, A. Chattopadhyay, Monitoring gramicidin conformations in membranes: a fluorescence approach, Biophys. J. 87 (2004) 831–843.
[23] A.K. Ghosh, R. Rukmini, A. Chattopadhyay, Modulation of tryptophan environment in membrane-bound melittin by negatively charged phospholipids: implications in membrane organization and function, Biochemistry 36 (1997) 14291–14305.
[24] M.C. Tory, A.R. Merrill, Determination of membrane protein topology by red-edge excitation shift analysis: application to the membrane-bound colicin E1 channel peptide, Biochim. Biophys. Acta 1564 (2002) 435–448.
[25] N.C. Santos, M. Prieto, M.A.R.B. Castanho, Interaction of the major epitope region of HIV protein gp41 with membrane model systems. A fluorescence spectroscopy study, Biochemistry 37 (1998) 8674–8682.
[26] H. Raghuraman, A. Chattopadhyay, Influence of lipid chain unsaturation on membrane-bound melittin: a fluorescence approach, Biochim. Biophys. Acta 1665 (2004) 29–39.
[27] F.G. Prendergast, Time-resolved fluorescence techniques: methods and applications in biology, Curr. Opin. Struct. Biol. 1 (1991) 1054–1059.
[28] W.B. De Lauder, Ph. Wahl, Effect of solvent upon the fluorescence decay of indole, Biochim. Biophys. Acta 243 (1971) 153–163.
[29] D.M. Rosenbaum, S.G.F. Rasmussen, B.K. Kobilka, The structure and function of G-protein-coupled receptors, Nature 459 (2009) 356–363.
[30] R. Heilker, M. Wolff, C.S. Tautermann, M. Bieler, G-protein-coupled receptor-focused drug discovery using a target class platform approach, Drug Discov. Today 14 (2009) 231–240.
[31] L. Anson, Membrane protein biophysics, Nature 459 (2009) 343.
[32] K. Rajarathnam, Designing decoys for chemokine–chemokine receptor interaction, Curr. Pharm. Des. 8 (2002) 2159–2169.